

Work functions, ionization potentials, and in-between: Scaling relations based on the image charge model

Kin Wong, Sascha Vongehr, and Vitaly V. Kresin

Department of Physics and Astronomy,

University of Southern California, Los Angeles, CA 90089-0484, USA

(Dated: June 14, 2021)

Abstract

We revisit a model in which the ionization energy of a metal particle is associated with the work done by the image charge force in moving the electron from infinity to a small cut-off distance just outside the surface. We show that this model can be compactly, and productively, employed to study the size dependence of electron removal energies over the range encompassing bulk surfaces, finite clusters, and individual atoms. It accounts in a straightforward manner for the empirically known correlation between the atomic ionization potential (IP) and the metal work function (WF), $IP/WF \sim 2$. We formulate simple expressions for the model parameters, requiring only a single property (the atomic polarizability or the nearest neighbor distance) as input. Without any additional adjustable parameters, the model yields both the IP and the WF within $\sim 10\%$ for all metallic elements, simulates the concentration dependence of the WF of regular binary bulk alloys, and matches the size evolution of the IP of finite metal clusters for a large fraction of the experimental data. The parametrization takes advantage of a remarkably constant numerical correlation between the nearest-neighbor distance in a crystal, the cube root of the atomic polarizability, and the image force cutoff length. The paper also includes an analytical derivation of the relation of the outer radius of a cluster of close-packed spheres to its geometric structure.

PACS numbers: 79.60.Jv, 78.67.-n, 61.46.+w

I. INTRODUCTION

While the good agreement between theoretical and experimental atomic ionization potentials (IP) is a major triumph for quantum mechanics, it is prohibitively more difficult to rigorously solve the polyatomic quantum problem, not to mention extrapolation to an infinite bulk metal. The IP for an atom is a well understood quantity. The same cannot, however, be said about the work function (WF) for a metal or even for a finite cluster. On the other hand, it is an experimentally realistic task to produce clusters ranging in size from two atoms up to tens of thousands of atoms and to measure the size dependence of the electron removal energy. The clusters can be made big enough that they can be considered close to bulk metals, hence the evolution from the atomic IP to the metal WF can be mapped out. Experiments over such a wide range have been performed, e.g., for sodium¹. For each element in the periodic table one would therefore expect that there exists a function which can predict the electron removal energy for a particle of arbitrary size.

The exact derivation of such a scaling law is a daunting task. However, the available experimental data on the IP, the WF, and on clusters reveal some characteristic features. For example, it has been noted a long time ago that the IP and the WF of metallic elements are approximately correlated to each other via the factor^{2,3}

$$I/W \approx 2. \tag{1}$$

To give another example, for many metal clusters of intermediate sizes the electron removal energy has been found to scale as

$$\phi \approx W + \gamma \frac{e^2}{R}, \tag{2}$$

where R is the radius of the cluster and γ is a constant factor^{4,5}. Henceforth, I will denote the atomic first ionization potential, W will denote the polycrystalline bulk surface work function, and for a finite metal particle the term "electron removal energy" will be employed (denoted by ϕ).

A significant number of first-principles calculations have been performed for work functions of metallic systems^{6,7,8}. In addition, simple models based on semi-empirical approaches combined with classical electrostatics have been rather successful at reproducing WF trends and values⁹. This suggests that some features of the desired scaling law may be found by employing such a model. In this paper we demonstrate that by combining the image-charge

potential function for a finite particle with just a single material-dependent scale parameter (the atomic polarizability α or the crystalline nearest-neighbor distance r_{nn}) one can obtain an interpolation formula covering the full size range from the atom through the cluster to the bulk. This formula estimates both the IP and the WF within $\sim 10\%$ for all metallic elements in the periodic table, yields values in reasonable agreement with experiment for many intermediate sized clusters, and provides a natural justification for the aforementioned $\text{IP}/\text{WF} \approx 2$ ratio.

The plan of the paper is as follows. In Sec. II we consider the image-charge expression which describes the removal of an electron from an isolated sphere. By focusing on the limits of a sphere of atomic radius and one of infinite radius, we show that the relation (1) follows as naturally from the image-charge consideration as does Eq. (2). In Sec. III we demonstrate some striking parallels between the variation of atomic sizes and image-force cutoff distances across the periodic table and use these observations to formulate compact expressions for estimating both WF and IP. An extension to the case of binary alloys is discussed in Sec. IV. Finally, we show that by using an appropriately interpolated expression for the cluster radius a good description of the size evolution of cluster ionization potentials can be obtained (Sec. V). Some rigorous formulas on close-packed cluster radii are derived in the Appendix.

II. THE IMAGE POTENTIAL MODEL

It is stated in the literature that the earliest attempt to explain the work function of a metallic surface using classical electrostatics was due to Debye¹⁰. He proposed that it is equal to the energy required to pull an electron out to infinity against its image charge. Since the image force diverges at the surface, Schottky¹¹ suggested that one may be able to define a microscopic cutoff distance d at which the image force starts to act. Despite the simplicity of this model¹², there have been numerous attempts to estimate the parameter d in order to fit the experimental values of the $\text{WF}^{2,3,9,13,14,15}$. Although the particular choices of d were supported only by plausibility arguments, they were frequently able to offer rather nice agreement with the experimental data.

In a similar spirit, let us now consider the image-force expression for the energy required to remove an electron from an isolated finite metal particle, modelled as a conducting sphere of radius R . The particle is assumed initially neutral, i.e., after the removal of the electron it

acquires an unit positive charge. A calculation of the work required to move the electron from a distance d outside the metal surface to infinity against its image charge is a straightforward exercise¹⁶:

$$\phi(R) = \frac{e^2}{4d} \left(\frac{1 + 4(d/R) + 6(d/R)^2 + 2(d/R)^3}{(1 + d/2R)(1 + d/R)^2} \right). \quad (3)$$

The cutoff parameter d is assumed to be a material-dependent constant. The first factor on the right-hand side represents the bulk ($R \rightarrow \infty$) work function: $W = e^2/(4d)$. This formula has been applied to yttrium and lanthanide clusters in Ref. [17]. However, the authors did not extend it to the bulk or the atomic limit; they used the equation as an extrapolation formula for small clusters with the WF as a given boundary condition.

It is convenient to rewrite the above equation in the following form:

$$\frac{\phi(R)}{W} = \eta(d/R), \quad (4)$$

where the dimensionless scaling function $\eta(d/R)$ is defined by the second factor in Eq. (3) and plotted in Fig. 1. If Eq. (4) were applied all the way down to the atomic limit, it would give an estimate of the ratio IP/WF as the value of $\eta(d/R_{at})$, where R_{at} is a quantity characterizing the atomic size. On the other hand, we know from numerous investigations^{2,3,9,13,14,15} that the cutoff parameter d is, sensibly enough, also of the same order of magnitude. In the atomic limit, therefore, the ratio d/R_{at} should be on the order of unity. In other words, if one assumes that $d \sim R_{at}$, then, independent of the exact expression for either parameter, the scaling function predicts that

$$I/W \sim \eta(1) \approx 2. \quad (5)$$

This is a new explanation of the well known empirical result mentioned in the Introduction, Eq. (1). In the next section we suggest some specific parametrizations of the variables d and R_{at} and show that these can give an even more accurate value of the IP/WF ratio.

In the large R limit, the scaling function can be expanded to first order in d/R . The result is:

$$\phi(R) = W + \frac{3e^2}{8R} + O\left(\left(\frac{d}{R}\right)^2\right). \quad (6)$$

This is the well known finite size correction for the ionization potential of metallic clusters^{4,5,18,19,20}. This scaling law has been experimentally verified for many metal clusters^{4,5,20,21}. Although there is still some controversy whether the 3/8 factor is sufficiently rigorous^{22,23,24,25,26}, Eq. (6) does fit the experimental data relatively well.

It appears, therefore, that Eq. (3) offers a consistent estimate for the scaling of electron removal energy from the atomic IP to finite particle sizes to the bulk WF. It is interesting to ask whether some simple parametrizations for the image force cutoff distance and atomic and cluster radii may be proposed so as to enable more quantitative applications of Eq. (3) to experimental data. This is the subject of the sections that follow.

III. LENGTH SCALE PARAMETERS

For guidance with length scaling, let us begin by plotting the "experimental" image force cutoff distances as defined by equating $e^2/(4d)$ to the experimentally measured bulk surface polycrystalline work functions²⁷. These values are shown in Fig. 2(a). The same figure displays two quantities reflecting the size of individual atoms: the cube root of the atomic polarizability²⁷ (r_α) and one-half of the nearest neighbor distance in a crystal²⁸ ($r_{nn}/2$). Although d shows strong correlation with both the polarizability radius and the nearest neighbor distance, it's consistently lower than either one. However, by forming the inverse sum of the two, a quantity emerges which follows the experimental values of d beautifully. This parametrization has the form

$$1/d \approx 1/r_\alpha + 2/r_{nn} \quad (7)$$

and agrees with the empirical value of the cutoff parameter to within $\sim 10\%$ for most metallic elements, see Fig. 2(b). Put another way, the WF for most metallic elements can be estimated to better than 10% by using this parametrization of d .

The coexistence of an atomic part and a bulk part in a work function model resembles qualitatively the elegant argument in Ref. [29] in which the WF value is calculated as arising from the IP of a neutral atom reduced by the work done by the image force in bringing the resulting ion back to the crystal surface.

As a matter of fact, Fig. 2(a) reveals that all the size parameters turn out to have essentially the same trend across the periodic table, differing only in overall magnitude. We are not aware of a quantitative theory explaining this observation for the crystalline state, but, roughly speaking, one does expect bigger atoms to have higher polarizabilities, larger lattice spacings in crystal form, and lower IP together with lower WF [via Eqs. (1,5)] and therefore greater d values. In fact, remarkably linear correlations between the

polarizability radius and such properties of individual atoms as the radius of the outermost orbital, the ionization potential, and the electronegativity have been extensively discussed in the literature (see Refs. 30,31,32 and references therein). This strongly suggests that just a *single* size parameter may be sufficient to yield an estimate for the WF.

Indeed, as shown in Fig. 3, it turns out that the ratio $r_{nn}/(2r_\alpha)$ is very close to 0.65 for all metallic elements³³ (the deviation from this average is within $\sim 20\%$), and this correlation can be substituted into Eq. (7). In the end, therefore, one can use, e.g., only the polarizability radius r_α in order to predict the approximate value of the bulk surface WF.

As shown in Fig. 4, a plot of

$$W = \frac{2.54e^2}{4r_\alpha}, \quad (8)$$

i.e., Eq. (7) with $r_{nn}/2 = 0.65r_\alpha$ [cf. Fig. 2(c)] confirms that this single-parameter formula gives WF estimates within $\sim 10\%$ of the experimental values. As mentioned at the beginning of Sec. II, a variety of expressions for the quantity d have been proposed earlier, but the one given here shares the virtues of needing only a single piece of information (the atomic polarizability or the nearest neighbor distance), being free of additional adjustable parameters, and producing rather accurate results.

Returning to the subject of the IP/WF ratio discussed in the previous section, Eq. (5), we notice that even more accurate agreement with the experimental average is obtained if we employ

$$d/R_{at} \approx r_{nn}/(2r_\alpha) \approx 0.65. \quad (9)$$

Indeed, this is a reasonable representation of the ratio of a characteristic crystalline length to an atomic length. This refinement gives

$$I/W \approx \eta(0.65) = 1.8, \quad (10)$$

see Fig. 3.

With estimates of both the work function WF, and the ratio IP/WF ≈ 1.8 , the atomic first ionization potential can be calculated. Fig. 5 shows the calculated IP plotted vs. the exact known IP²⁷. The accuracy is again $\pm 10\%$ for most elements³⁴.

Eqs. (7) and (9) imply the following expression for the size parameter R_{at} in the atomic limit:

$$R_{at} \approx \frac{r_\alpha^2}{r_\alpha + r_{nn}/2} \approx 0.61r_\alpha, \quad (11)$$

where in the last part we again used the average experimental ratio between r_{nn} and r_α .

The discussion in this section shows that a consistent and economical description of electron removal energies both in the bulk and the atomic limits can be achieved with the help of only a single atomic parameter. In the next section we will consider the region in between, i.e., the electron removal energies for clusters of a finite number of atoms.

IV. ESTIMATE OF ALLOY WORK FUNCTIONS

The regularities discussed above have been deduced for pure metals. It is interesting to inquire what they might imply for mixed systems such as binary alloys. Obviously, it is beyond the capacity of the present approach to achieve a microscopic understanding of mixed systems and to incorporate the possible variations in structure and miscibility. Nevertheless, it makes sense to consider a simple scaling argument for continuous bulk solutions.

The preceding section demonstrated that the WF can be rather accurately parametrized as being inversely proportional either to the polarizability radius or to the nearest-neighbor distance. In an alloy A_xB_{1-x} the effective values of these length parameters will change. In fact, there are two natural approximations which can be made. One is that the lattice parameter will change linearly with concentration. This is known as Vegard's law^{8,35}. Within the framework of the present model, the alloy WF would then behave as the inverse average of the constituents' WF's: $1/W(x) \approx x/W_A + (1-x)/W_B$.

An alternative and possibly more physical assumption is that it is the effective polarizability that should be taken as varying linearly with concentration. Indeed, the polarizability of a small volume element of the sample is approximately the weighted average of the polarizabilities of the components. In this case, with $W \sim \alpha^{-1/3}$, we anticipate

$$\frac{1}{[W(x)]^3} = \frac{x}{W_A^3} + \frac{1-x}{W_B^3} \quad (12)$$

Note that this relation would also be obtained if we assumed that it was the molar volumes, rather than lattice parameters, that would need to be averaged upon alloying (Zen's law^{8,36}).

Well-controlled measurements of $W(x)$, like rigorous calculations, are not many in number: traces of surface segregation or contamination can obliterate the basic effect. Fig. 6 illustrates the prediction of Eq. (12) for binary alloys of silver and gold, carefully charac-

terized in Ref. 37. The scaling curve reproduces the trend of the data and even the correct curvature of the Ag-Au line. It is noteworthy that predicting the sign of the deviation of $W(x)$ from linearity appears to be a difficult challenge for microscopic theory. The one calculation which focused on such a deviation³⁸ applied a self-consistent two-band charge-transfer model to Ag_xAu_{1-x} and was able to yield the correct sign only when level shifts due to alloying were taken into account. The absolute magnitude of the calculated deviation was approximately one-third of the experimental value, and was in fact very close to the curve in Fig. 6 produced by Eq. (12).

For cases when the constituents' work functions differ by relatively small amounts, such as alkali alloys^{39,40}, (Eq. (12) predicts an essentially linear interpolation, in agreement with the data.

It is seen, therefore, that scaling estimates can be usefully applied to the work functions of smoothly evolving alloys. Of course, cases when the WF is not a monotonic function of concentration^{40,41} call for more involved structural and theoretical analysis.

V. ELECTRON REMOVAL ENERGIES FOR CLUSTERS AND HARD SPHERE PACKING

Having shown that the scaling law, Eq. (3), offers good guidance for both IP and WF, we now address the intermediate regime of finite clusters. Therefore a workable parametrization of cluster radius, R_{cl} , is needed for use in this equation.

A commonly used method to estimate the particle radius is to scale it according to the Wigner-Seitz radius: $R_{cl}(N) = r_s N^{1/3}$, where N is the number of atoms. This expression, commonly augmented with an electron spill-out term, has been used to describe many cluster properties. However, if this formula is used in Eq. (3) together with the expressions for d obtained above, a close match with the experimental data is not obtained. Moreover, it is desirable to retain a form that would depend only on N and on the parameters r_α and/or r_{nn} , as in the atomic and bulk limits described above.

A complementary definition of cluster radius has been proposed in Ref. [17,42]. The cluster was modelled as a group of hard spheres packed so as to minimize the surface area. The radius of a sphere circumscribing the close-packed cluster was then substituted into Eq. (3). By packing steel balls in a rubber envelope, the authors found empirically that this

circumscribing sphere radius could be expressed as

$$R_{cl}(N) \approx 1.3r_0N^{1/3} \quad (13)$$

for clusters $N \gtrsim 7$, where r_0 is the radius of each individual hard sphere. For smaller clusters, the exact circumscribing sphere radius can be derived from simple geometry¹⁷. This definition gave reasonable answers for several metal clusters, although additional adjustable parameters had to be employed. We found that an expression of the type (13) can be derived analytically for various cluster packing arrangement. The precise numerical coefficient varies with the packing structure, but in all cases is not far from 1.3. The analysis is described in the Appendix.

Based on these considerations, we formulate the following interpolation for the parameter R to be used in Eq. (3) for the calculation of clusters' $\phi(R)$:

$$R \approx \frac{R_{cl}^2(N)}{R_{cl}(N) + r_{nn}/2}. \quad (14)$$

Here $R_{cl}(N)$ is the outer, or circumscribing (as described above) radius for a cluster with N hard spheres, each of a radius equal to the polarizability radius $r_0 = r_\alpha$. As before, r_{nn} is the nearest neighbor distance of the bulk metal. For $N \gg 1$ this expression turns into R_{cl} ⁴³, while in the atomic limit it is the same as Eq. (11).

In view of the previously discussed relation between the experimental values of r_{nn} and r_α , this equation can be rewritten purely in terms of the latter quantity. In particular, for the larger clusters for which Eq. (13) holds, we obtain

$$R \approx \frac{1.3r_\alpha N^{1/3}}{1 + 0.5N^{-1/3}} \quad (15)$$

When these expressions are used together with d from the previous section in Eq. (3) [note that for the smallest clusters it is important to use the full image-charge formula rather than the expansion (6)], they succeed in describing the behavior of a large fraction of elemental metallic clusters. This is shown in Fig. 7 which compares the calculated electron removal energies with experimental results on clusters for which data over a sufficient size range are available. It is not surprising that the cluster fits are not of uniform quality⁶¹. Indeed, whereas our aim has been to reduce as much as possible the number of input parameters, the definition of cluster size is inherently not so "universal." The geometric structures of clusters containing up to several hundred atoms are neither constant nor necessarily the

same as the bulk limit (see, e.g., the reviews in Refs. 62,63), and the bond lengths may generally vary both with cluster size and from the inner to the outer layers. As a result, the formulae given in this section should be viewed as approximations. Their utility is in the fact that they provide a sensible interpolation between the atomic and bulk limits discussed above, and it is satisfying that a one-parameter expression in many cases provides not only qualitative but also quantitative guidance.

VI. SUMMARY

The main results of this work can be summarized as follows.

(1) Starting with an expression for the electron removal energy in terms of the image charge potential for an isolated spherical particle and a surface cutoff parameter [Eq. 3], we explored how this model may be consistently applied to metallic systems ranging from bulk surfaces to finite clusters and down to individual atoms.

(2) We showed that this approach provides a transparent physical explanation for the empirical fact that the atomic ionization potentials and polycrystalline work functions of the metallic elements exhibit an almost constant ratio of ~ 2 over the periodic table [Eqs. (1, 10)].

(3) We found that for most elements there is a remarkably close numerical correlation between the values of the nearest-neighbor distance in a crystal, the cube root of the atomic polarizability, and the image force cutoff parameter. This correlation may be rationalized qualitatively, but appears worthy of further study.

(4) Taking advantage of this correlation, we formulated simple expressions for the cutoff distance [Eq. (7)] and the atomic and cluster radii [Eqs. (11,14,15)]. They yield good estimates for the work function, the ionization potential, and the cluster electron removal energies by using only a *single input parameter*, the atomic polarizability. No extra adjustable parameters are required.

(5) Generalizing the scaling argument to the case of binary alloys, we found that it can simulate the shape of the concentration dependence of work functions of continuous bulk solutions [Eq. (12)].

(6) We also provided an analytical derivation of the connection between the geometric structure of a cluster of close-packed spheres and its outer radius. It is described by an

equation of the type (13), but the precise numerical coefficient is shown to depend on the packing structure.

Acknowledgments

We are grateful to Prof. Walter E. Harrison, Dr. Tomasz Durakiewicz, and Dr. Leeor Kronik for very informative discussions, and to the referee for useful suggestions. This work was supported by the U.S. National Science Foundation under Grant No. PHY-0098533.

APPENDIX: HARD SPHERE PACKING

There exist well-defined geometries for finite systems which provide densely packed structures corresponding to specific bulk lattices in the large-size limit. As reviewed in detail, e.g., in Refs. [64,65,66], these structures are best visualized as arising from the packing of spheres. Some of the commonly encountered ones are illustrated in Fig. 6. Here we derive the outer radii of these structures as a function of the number of hard spheres, N . The radius is defined as corresponding to the *smallest sphere which completely encloses (circumscribes)* the cluster made up of N close-packed hard spheres, each with a radius r_0

1. Cubeoctahedron

The cubeoctahedron is a shape with small surface area which can be cut out of an *fcc* crystal. The number of hard spheres as a function of the number of shells k is given by⁶⁵ $N = (10/3)k^3 - 5k^2 + (11/3)k - 1$. The outer radius R is given by $R = (2k - 1)r_0$. For large k this becomes $R \approx 2kr_0 \approx 2(3/10)^{1/3}r_0N^{1/3} \approx 1.339r_0N^{1/3}$. The same expression can be derived by evaluating the volume of the circumscribing sphere relative to the sum of the volumes of the small hard spheres⁶⁷.

2. Truncated hexagonal bipyramid

The truncated bipyramid arises from an *hcp* lattice. The number of hard spheres in a truncated bi-pyramid is $N = -(3/4) + (7/2)k - (21/4)k^2 + (7/2)k^3$ for odd k and $N = -1 + (7/2)k - (21/4)k^2 + (7/2)k^3$ for even k . The outer radius is $R = (2k - 1)r_0$. For large k , $R \approx 2(2/7)^{1/3}r_0N^{1/3} \approx 1.317r_0N^{1/3}$.

3. Rhombic dodecahedron

The rhombic dodecahedron derives from *bcc*. The number of hard spheres in a rhombic dodecahedron is $N = 4k^3 - 6k^2 + 4k - 1$, and the outer radius is $R = (4/\sqrt{3}(k - 1) + 1)r_0$. For large k , $R \approx 4/\sqrt{3}(1/4)^{1/3}r_0N^{1/3} \approx 1.455r_0N^{1/3}$.

4. Icosahedron

The icosahedron has the highest symmetry of all discrete point groups. Although due to its five-fold symmetry, the icosahedron does not form bulk crystals, it can be considered as a slightly distorted fcc crystal. The icosahedron structure has been observed for small clusters of inert-gas clusters, Ca, and Mg clusters (see references in 65). The relationship between the number of hard spheres and the number of shells is the same as for the cube-octahedron⁶⁵: $N = (10/3)k^3 - 5k^2 + (11/3)k - 1$. The radius is also given by the same expression as for the cube-octahedron $R = (2k - 1)r_0$. The resulting expression for the cluster radius is therefore the same as for the cube-octahedron. For large k the radius is: $R \approx 2kr_0 \approx 2(3/10)^{1/3}r_0N^{1/3} \approx 1.339r_0N^{1/3}$.

-
- ¹ H. Göhlich, T. Lange, T. Bergmann, U. Näher, and T. P. Martin, Chem. Phys. Lett. **187**, 67 (1991).
- ² C. F. Gallo and W. L. Lama, IEEE Trans. Ind. Appl. **1A-10**, 496 (1974).
- ³ A. Rose, Solid State Comm. **45**, 859 (1983).
- ⁴ M. Seidi, K. -H. Meiwes-Broer, M. Brack, J. Chem. Phys. **95**, 1295 (1991).
- ⁵ W. A. de Heer, Rev. Mod. Phys. **65**, 611 (1993).
- ⁶ N.D.Lang, in *Theory of the Inhomogeneous Electron Gas*, ed. by S.Lundqvist and N.H.March (Plenum, New York, 1983).
- ⁷ K.Jacobi, in *Landolt-Börnstein Numerical Data and Functional Relationships in Science and Technology*, Group III, Vol. 24, subvol. *b*, ed. by G. Chiarotti (Springer, Berlin, 1994).
- ⁸ A.Kiejna and K.F.Wojciechowski, *Metal Surface Electron Physics* (Elsevier, Oxford, 1996).
- ⁹ T. Durakiewicz, S. Halas, A. Arko, J. J. Joyce, and D. P. Moore, Phys. Rev. B **64**, 045101 (2001).
- ¹⁰ P. Debye, Ann. Phys. **33**, 441 (1910).
- ¹¹ W. Schottky, Zeits. Phys. **14**, 63 (1923).
- ¹² Since electrons in a metal are actually delocalized, a more rigorous justification may be to consider the WF as the work involved in modifying the electron density distribution. Viewing the electron cloud as spilling out to an effective boundary a distance d from the surface, the work function can be identified with the difference in electrostatic energy between point d and infinity.
- ¹³ I. Brodie, Phys. Rev. B **51**, 13660 (1995).
- ¹⁴ S. Halas and T. Durakiewicz, J. Phys. Condens. Matter **10**, 10815 (1998).
- ¹⁵ K.F. Wojciechowski, A. Kiejna, and H. Bogdanow, Mod. Phys. Lett. B, **13**, 1081 (1999).
- ¹⁶ J. D. Jackson, *Classical Electrodynamics*, 3rd ed. (Wiley, New York, 1998).
- ¹⁷ T. Durakiewicz and S. Halas, Chem. Phys. Lett. **341**, 195 (2001).
- ¹⁸ J. M. Smith, AIAA J. **3**, 648 (1965).
- ¹⁹ D. M. Wood, Phys. Rev. Lett. **46**, 749 (1981).
- ²⁰ C. Bréchnac, in *Clusters of Atoms and Molecules*, Vol. I, ed. by H. Haberland (Springer, Berlin, 1994).

- ²¹ Ph. Dugourd, D. Rayane, P. Labastie, B. Vezin, J. Chevalerey and M. Broyer, *Chem. Phys. Lett.* **197**, 433 (1992).
- ²² G. Makov, A. Nitzan, and L. E. Brus, *J. Chem. Phys.* **88**, 5076 (1988).
- ²³ W. A. de Heer and P. Milani, *Phys. Rev. Lett.* **65**, 3356 (1990).
- ²⁴ M. K. Harbola, *J. Chem. Phys.* **97**, 2578 (1992).
- ²⁵ M. Seidl and J. P. Perdew, *Phys. Rev. B*, **50** 5744 (1994).
- ²⁶ C. Yannouleas and U. Landman, in *Large Clusters of Atoms and Molecules*, ed. by T. P. Martin (Kluwer, Dordrecht, 1996).
- ²⁷ *CRC Handbook of Chemistry and Physics*, ed. by D. R. Lide, 82nd ed.(CRC Press, Boca Raton, 2001).
- ²⁸ C. Kittel, *Introduction to Solid State Physics*, 7th ed. (Wiley, New York, 1996).
- ²⁹ W. A. Harrison, *Elementary Electronic Structure* (World Scientific, Singapore, 1999), Sec. 19-2.
- ³⁰ I.K.Dmitrieva and G.I.Plindov, *Phys. Scr.* **27**, 402 (1983).
- ³¹ J.K.Nagle, *J. Am. Chem. Soc.* **112**, 4741 (1990).
- ³² T.K.Ghanty and S.K.Ghosh, *J. Phys. Chem.* **100**, 17429 (1996).
- ³³ Within individual structural families, the average of the ratio $r_{nn}/(2r_{\alpha})$ is 0.72 for the *fcc* metals, 0.66 for the *hcp* metals, and 0.61 for the *bcc* metals.
- ³⁴ It may be noted in both Figs. 4 and 5 that elements with three valence electrons account for a large fraction of deviations (B-Al-Ga-In-Tl) as well as for the switched ordering of the IPs of the sequence Sc-Y-La. The present semi-empirical level is not designed to pinpoint the origin of such behavior, but it is a compelling question for further research.
- ³⁵ L.Vegard, *Z.Phys.* **5**, 17 (1921).
- ³⁶ E.Zen, *Amer. Mineral.* **41**, 523 (1956).
- ³⁷ S.C.Fain, Jr. and J.M.McDavid, *Phys. Rev. B* **9**, 5099 (1974).
- ³⁸ C.D.Gelatt, Jr. and H.Ehrenreich, *Phys. Rev. B* **10**, 398 (1974).
- ³⁹ Th.G.J. van Oirschot, M. van den Brink, and W.M.H.Sachtler, *Surf. Sci.* **29**, 189 (1972).
- ⁴⁰ Ju.I.Malov, M.D.Shebzukhov, and V.B.Lazarev, *Surf. Sci* **44**, 21 (1974).
- ⁴¹ R.Ishii, K.Matsumura, A.Sakai, and T.Sakata, *Appl. Surf. Sci.* **169-170**, 658 (2001).
- ⁴² T. Durakiewicz, S. Halas, and J. J. Joyce, to be published.
- ⁴³ In the limit of large clusters which can be thought of as bulk crystal fragments, the radii of their circumscribing spheres should become proportional to r_{nn} rather than r_{α} , which implies

an additional numerical factor in Eq. (14). However, in the small-cluster limit for which most experimental data are available and for which we are developing a parametrization, the use of r_α gives a better fit. As remarked at the end of Sec. V, this evidently reflects the fact that the small metal clusters, produced in beam sources, do not necessarily possess the exact bulk geometry.

- ⁴⁴ M. M. Kappes, S. Schär, U. Röthlisberger, C. Yeretjian, and E. Schumacher, *Chem. Phys. Lett.* **143**, 251 (1988).
- ⁴⁵ J. L. Persson, Ph.D. Dissertation, University of California, Los Angeles, 1991
- ⁴⁶ M. L. Homer, J. L. Persson, E. C. Honea, and R. L. Whetten, *Z. Phys. D* **22**, 441 (1991).
- ⁴⁷ W. A. Saunders, K. Clemenger, W. A. de Heer, and W. D. Knight, *Phys. Rev. B* **32**, 1366 (1985).
- ⁴⁸ W. A. Saunders, Ph.D. Dissertation, University of California, Berkeley, 1986.
- ⁴⁹ M. Knickelbein, *J. Chem. Phys.* **102**, 1 (1994).
- ⁵⁰ M. B. Knickelbein and S. Yang, *J. Chem. Phys.* **93**, 5760 (1990).
- ⁵¹ G. M. Koretsky and M. B. Knickelbein, *J. Chem. Phys.* **106**, 9810 (1997).
- ⁵² S. Yang and M. B. Knickelbein, *J. Chem. Phys.* **93**, 1533 (1990).
- ⁵³ M. B. Knickelbein, S. Yang, and S. Riley, *J. Chem. Phys.* **93**, 94 (1990).
- ⁵⁴ M. B. Knickelbein, *Chem. Phys. Lett.* **192**, 129 (1992).
- ⁵⁵ C. Jackschath, I. Rabin, and W. Schulze, *Z. Phys. D* **22**, 517 (1992).
- ⁵⁶ M. Ruppel and K. Rademann, *Chem. Phys. Lett.* **197**, 280 (1992).
- ⁵⁷ K. E. Schriver, J. L. Persson, E. C. Honea, and R. L. Whetten, *Phys. Rev. Lett.* **64**, 2539 (1990).
- ⁵⁸ M. Pellarin, J. Lermé, B. Baguenard, M. Broyer and L. Vialle, *Ber. Bunsenges. Phys. Chem.* **96**, 1212 (1992).
- ⁵⁹ S. Yoshida and K. Fuke, *J. Chem. Phys.* **111**, 3880 (1999).
- ⁶⁰ G. M. Koretsky and M. B. Knickelbein, *Eur. Phys. J. D* **2**, 273 (1998).
- ⁶¹ Of the six elements that deviate the most from the scaling curves, two (Li, Mn) have a ratio $r_{mn}/(2r_\alpha)$ which is significantly different from the average value of 0.65 and one (Sn) does not have a closed-packed crystal structure. Furthermore, note that even the strongest deviations in Fig. 7 are less than 20%.
- ⁶² *Clusters of Atoms and Molecules*, Vols. I and II, ed. by H. Haberland (Springer, Berlin, 1994).

- ⁶³ M. B. Knickelbein, *Philos. Mag.* **79**, 1379 (1999).
- ⁶⁴ H. Müller, H.-G. Fritsche, and L. Skala, in *Clusters of Atoms and Molecules*, Vol. I, ed. by H. Haberland (Springer, Berlin, 1994).
- ⁶⁵ T. P. Martin, *Phys. Rep.* **273**, 299 (1996).
- ⁶⁶ B. M. Smirnov, *Clusters and Small Particles* (Springer, New York, 2000).
- ⁶⁷ K. L. Wong, Ph.D. Dissertation, University of Southern California, 2002.

Figures

FIG. 1: A plot of the scaling function $\eta(d/R)$ governing the variation of the electron removal energy with size, see Eq. (4).

FIG. 2: Diamonds: the experimental work functions²⁷ plotted in terms of $d = e^2/(4W)$. (a) Triangles: r_α , the cube root of the atomic polarizability; circles: $r_{nn}/2$, one-half of the crystalline nearest neighbor distance. (b) Squares: Eq. (7) for the parameter d . (c) Circles: $r_\alpha/2.54$.

FIG. 3: Stars: a plot of the ratio $r_{nn}/(2r_\alpha)$ for the metallic elements (the average is ≈ 0.65). Diamonds: the ratio IP/WF (the average is ≈ 1.8).

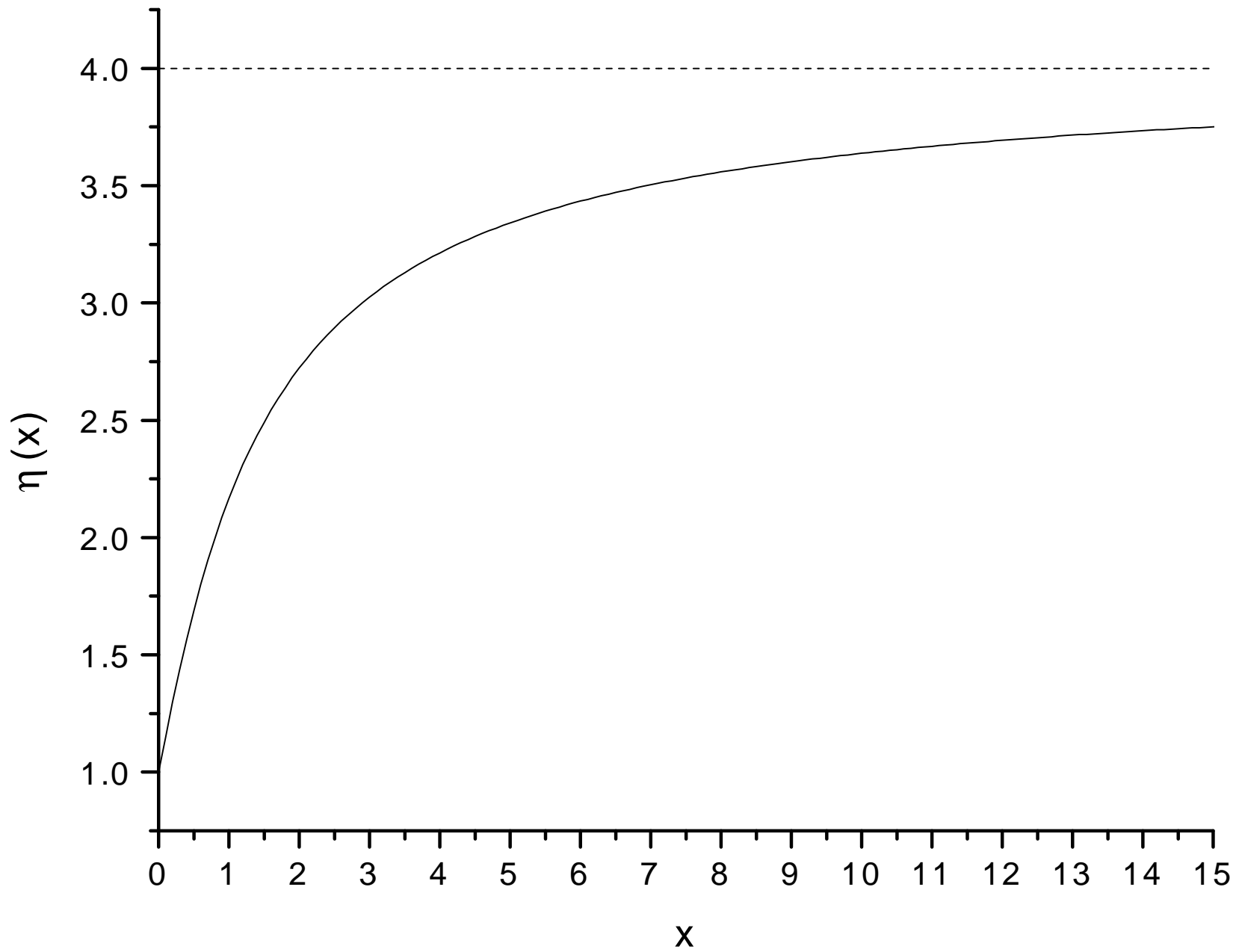
FIG. 4: A plot of metal work functions estimated by Eq. (8) vs. the experimental values. The straight lines mark the region of $\pm 10\%$ deviation.

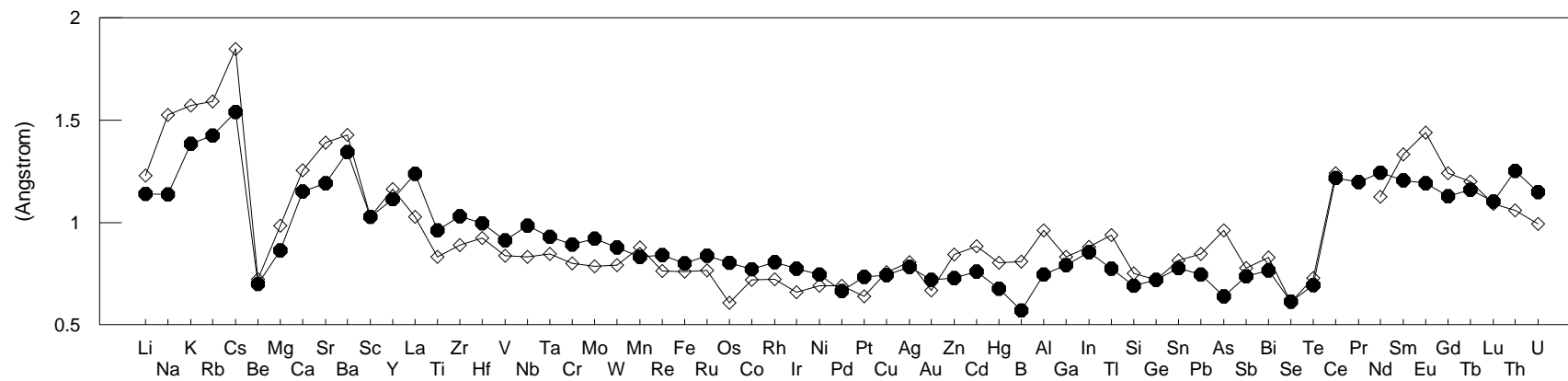
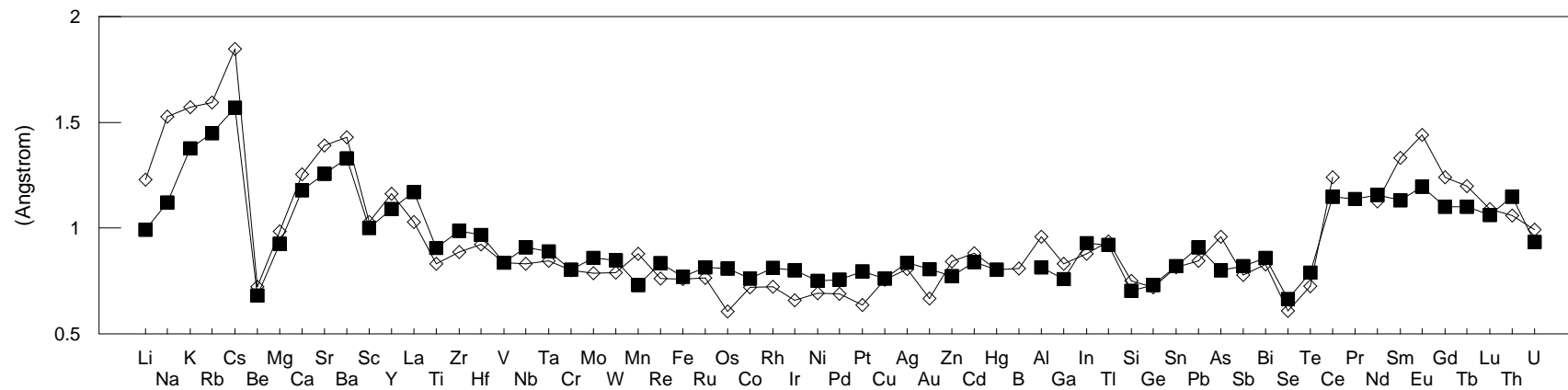
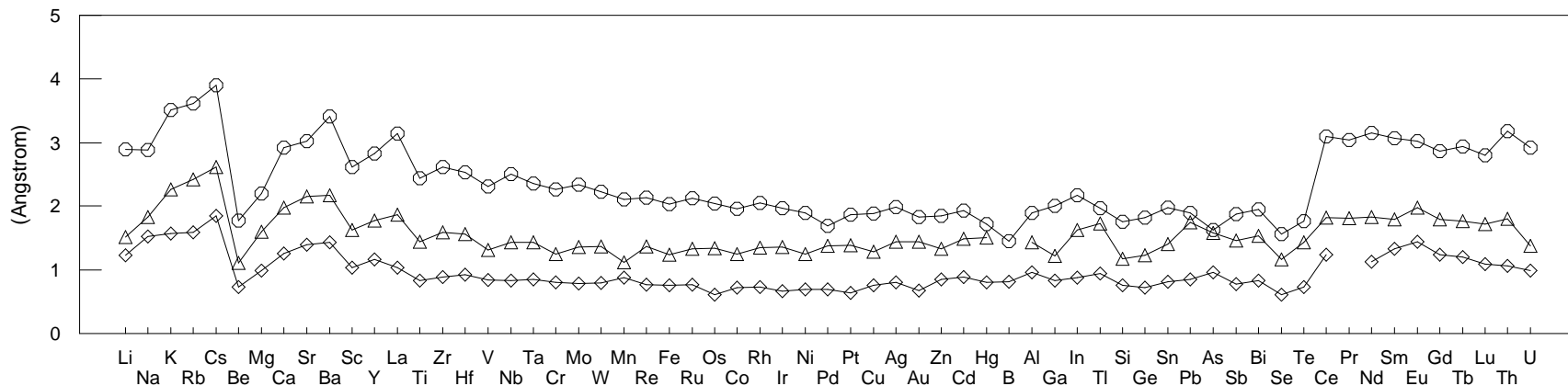
FIG. 5: A plot of atomic ionization potentials estimated by Eqs. (8,10) vs. the experimental values²⁷. The straight lines mark the region of $\pm 10\%$ deviation.

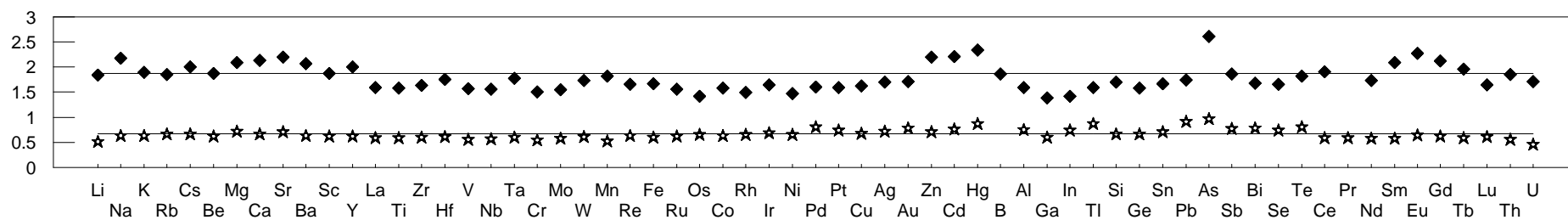
FIG. 6: Concentration dependence of the work function of Ag-Au binary alloys. Solid line: estimate according to Eq. (12), dotted line: experimental behavior³⁷, dashed line: linear interpolation.

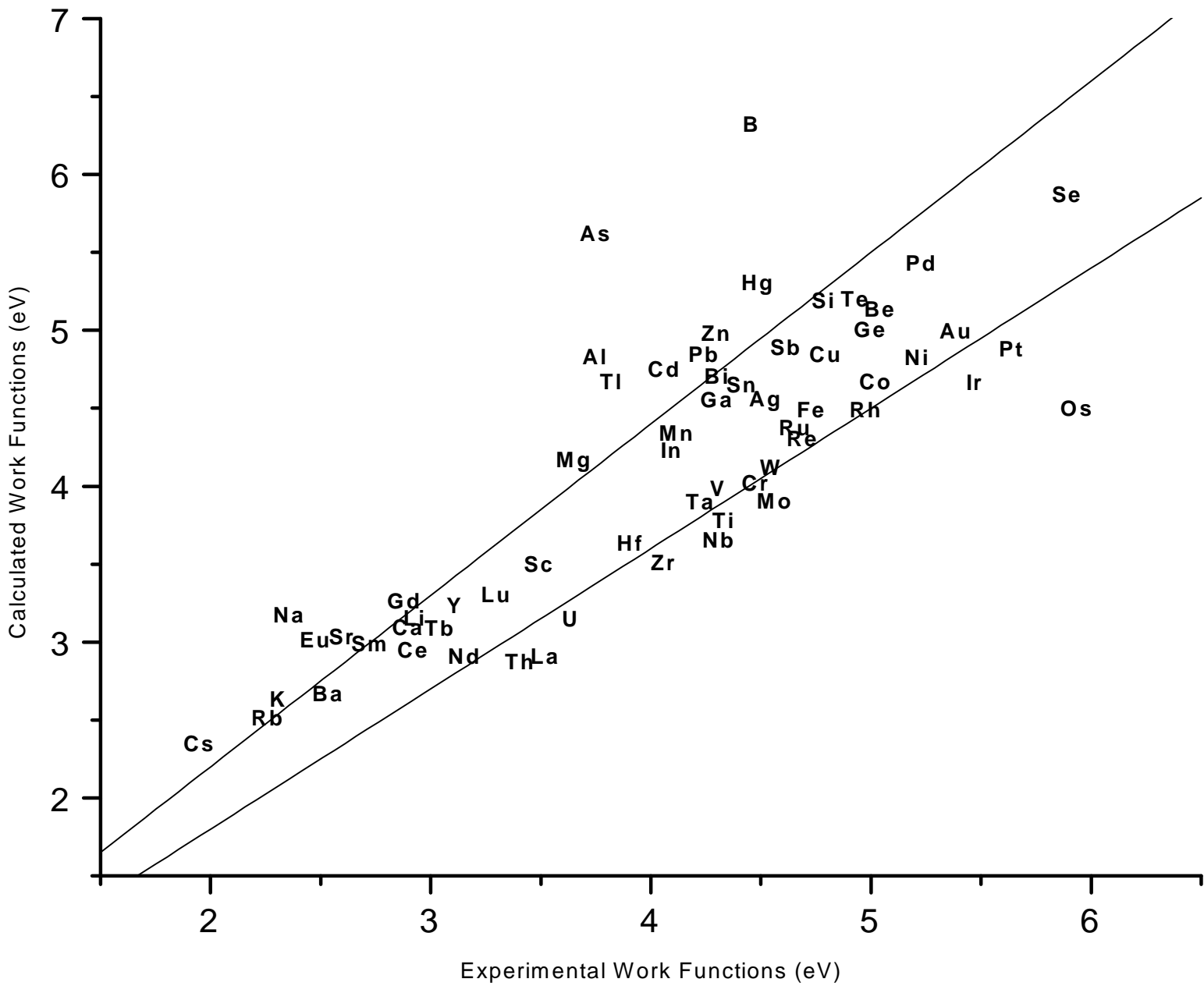
FIG. 7: A comparison between the experimental electron removal energies of small metal clusters (dots) and the model described in the text (solid curves). The first (circled) dot in each plot is the atomic ionization potential. The data were adapted from Refs. [21] (Li), [44,45,46] (Na), [47,48] (K), [49] (Y), [50] (Nb), [51] (Mn), [52] (Fe), [52] (Co), [53] (Ni), [54] (Cu), [55] (Ag), [56] (Cd), [57] (Al), [58] (In), [59] (Sn), and [60] (Ce,Pr).

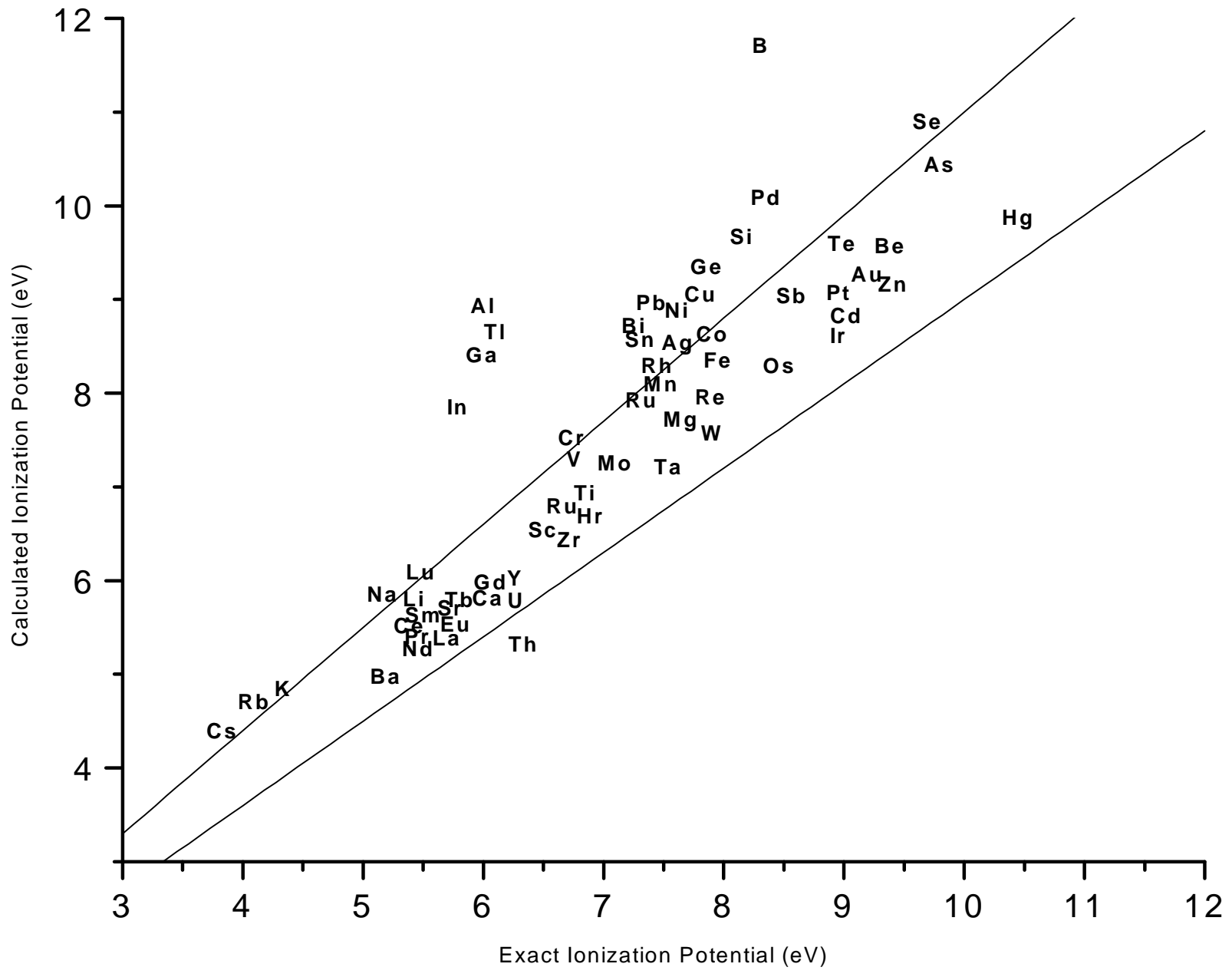
FIG. 8: Hard-ball and polyhedral depictions of close-packed structures: (a) Cubeoctahedron, (b) Rhombic dodecahedron, (c) Truncated hexagonal bipyramid, (d) Icosahedron.

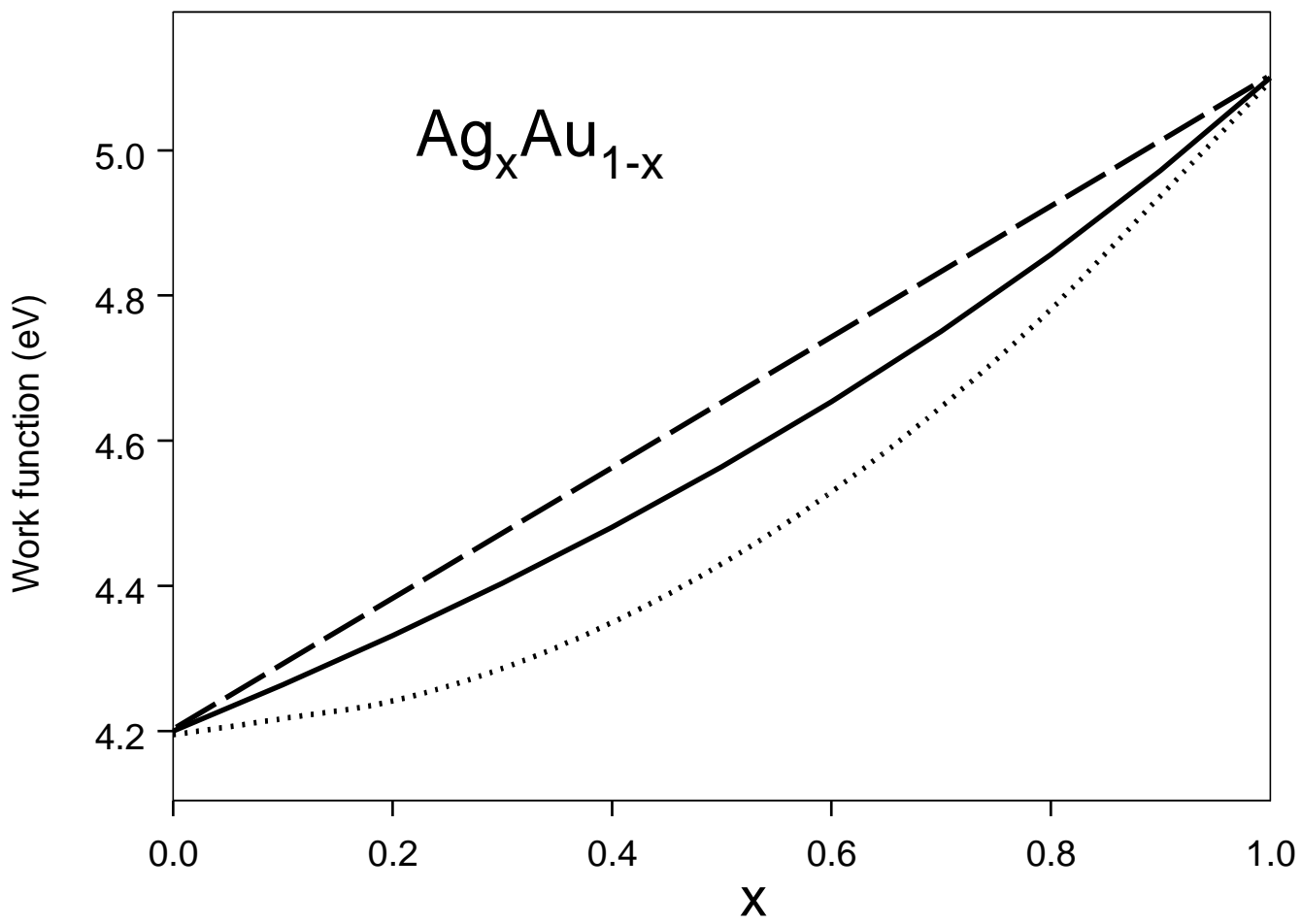


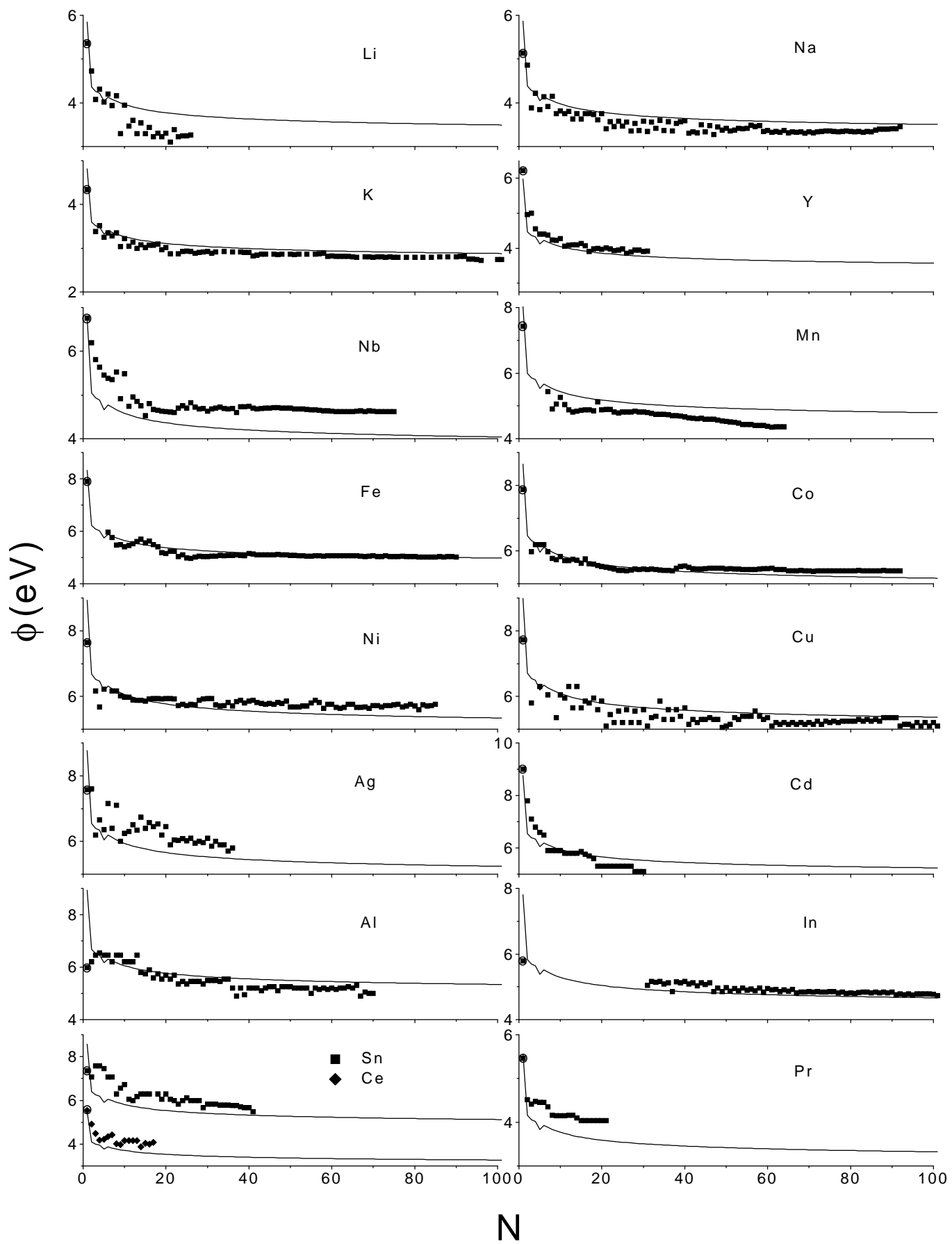




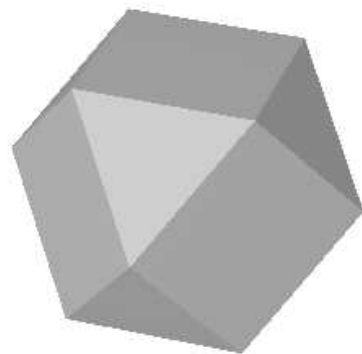
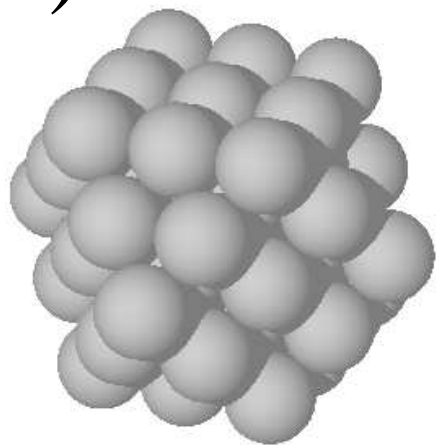




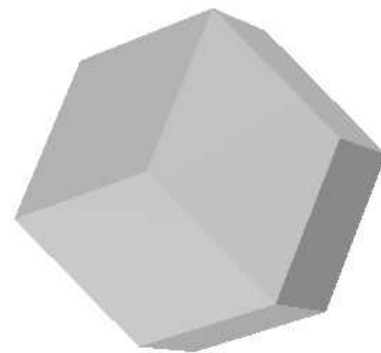
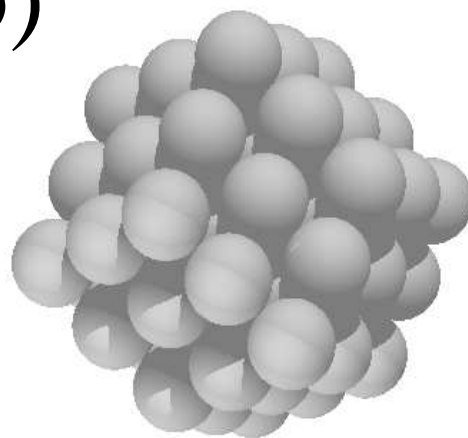




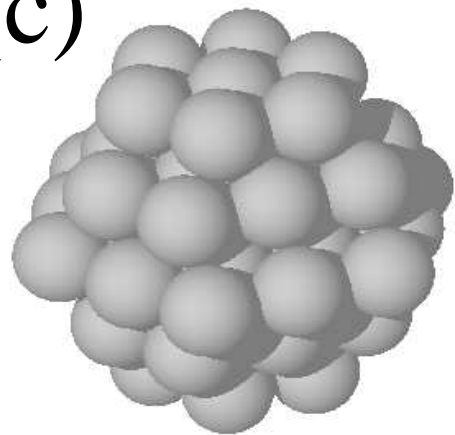
(a)



(b)



(c)



(d)

